2009 American Control Conference
Hyatt Regency Riverfront, St. Louis, MO, USA
June 10-12, 2009

Petri nets control design for hybrid electrical energy systems

Alioune Badara MBOUP[1,2], François GUERIN[1], Pape Alioune NDIAYE[2] and Dimitri LEFEBVRE[1]
[1]GREAH – University Le Havre, 25 rue Philippe Lebon, 76058 Le Havre Cedex, France
[2]CIFRES – Ecole Supérieure Polytechnique UCAD Dakar, Senegal
{francois.guerin ; dimitri.lefebvre} @univ-lehavre.fr ;{abmboup; pndiaye} @ucad.sn

Abstract- **This paper describes a supervisory control strategy based on Petri nets for electrical energy transfers in multisource renewable energy systems. The aim is to optimize the energy transfers, according to the sources power variations and the load characteristics. For this purpose, the proposed Petri net controller calculates the operating mode of the multisource renewable energy system. This high level controller is combined with a low level one that tunes the power ratio provided by each source according to sources power (climatic conditions) and load variations. An estimation of the duty cycle value of the dc/dc power converters is used to fire the Petri nets transitions, to switch the power sources and also to drive the power ratios.**

I. INTRODUCTION

Electrical energy is an essential factor for the development of human societies. The limited reserves of fuel oils and their unstable prices have significantly increased the interest in renewable energy sources. That's why the design of Systems of Multiple Sources of Energy (SMSE) has received considerable attention in the last decade [1]. Such systems constitute the most economical solution in many applications. In addition, they may result in lower environmental pollution and provide a more reliable supply of electricity through the combination of several energy sources [2]. Hybrid energy systems frequently combine solar and wind energy sources with a lead-acid batteries or fuel cells (to overcome periods of scarce generation).

Recently, several researches [3], [4], [5] have focused on control of hybrid power sources according to the measurement of the main significant variables (solar radiations, wind turbine shaft speed…). These methods are mainly designed as a combination of several local controllers and require the use of additive sensors to be efficient. The main contribution of this paper is to propose an alternative solution to design supervisory control for hybrid energy systems based on Petri nets (PN). PN are useful for the study of discrete event systems (DES) [21] and hybrid dynamical systems (HDS) [28] because they combine, in a comprehensive way, intuitive graphical representations and powerful analytic expressions [19], [20], [24]. As a consequence, a lot of results based on PN theory have been established for the control design of DES and HDS. One of the most famous approaches concerns the supervisory control where the system and the controller are considered as DES [23], [25], [27].

A PN control approach is developed in this paper. The coupling of one or several sources in SMSE will be considered as a DES to be controlled according to the climatic conditions and load variations. For this purpose, Petri nets are introduced. Another reason to use PN is that continuous and discrete dynamics are combined in hybrid power systems: mode commutations and continuous variations of electrical variables influence each other. PN models are well known as an efficient tool for the modeling, analysis and control of HDS [28]. From our knowledge, only few contributions exist concerning the use of PN for hybrid power systems. Timed PN have been investigated to analyze a maximum power point tracking (MPPT) converter [29], and differential and hybrid PN have been recently introduced to model and simulate hybrid power systems [30], [31]. In comparison, our contribution focuses on control design. The proposed control scheme is based on a reliable and accurate multimodel for the coupling of several dc/dc power converters on a dc bus [6]. The supervisory control has two levels: the high level based on PN determines the operating mode of the multisource renewable energy system; the low level based on continuous controllers drives the power ratio provided by each source. Both levels use the duty cycle value (dc/dc power converters) as decision criteria. As a consequence, the selection of operating mode and the local control design are presented in a framework with the advantage that the proposed supervisory control doesn't need extra sensors to measure the available sources power.

II. MODELING OF HYBRID ENERGY SYSTEMS

A. Topology of the mutisource energy system

The multisource renewable energy system, studied in this paper, is represented on Fig.1. It is made up of a diesel generator, a photovoltaic module, a wind turbine, a storage battery and a variable load. All these elements are connected onto a dc bus via identical Zero Voltage Switched (ZVS) full bridge isolated buck converters. GREAH laboratory of the University Le Havre (France) develops an experimental center similar to the studied topology on the site of *Fecamp* (http://lycees.ac-rouen.fr/maupassant/ site2/article325.html).

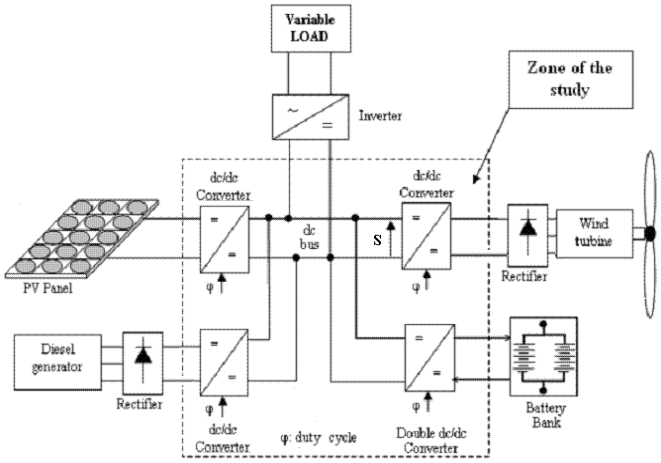

Fig.1: Topology of the multisource renewable energy system.

In order to optimize the energy transfers according to the sources power variations and the load characteristics, the authors have designed an average state space model that brings a detailed physical explanation of the coupling and uncoupling of several identical dc/dc power converters on a dc bus [6]. The proposed multimodel consists in a mathematical generic expression whose parameters change according to the dc/dc power converters coupled on the dc bus. It takes into account conduction losses in dc/dc power converters and is adapted to the case of different dc/dc power converters (forward, flyback…).

B. Model of a dc/dc power converters coupled onto a dc bus

The structural diagram of the ZVS full bridge isolated buck converter [7], [8], [9] is represented on Fig.2. We suppose that it runs in continuous conduction mode. The full bridge control (Q1 to Q4) is realized by a phase shift controller UC3879. The duty cycle value φ is modified by the phase shift between V_A and V_B voltages. The coupling of the dc/dc power converter is obtained by the closing of the contactor M (close: M=1, open: M=0).

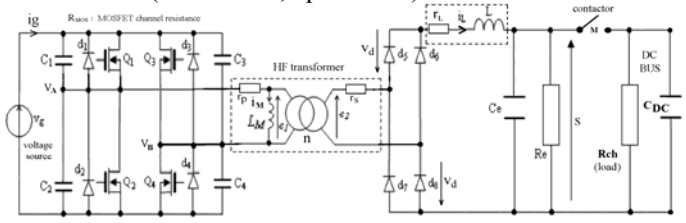

Fig.2: Structural diagram of the ZVS full bridge isolated buck converter

Four running phases must be distinguished according to the switches Q_1 to Q_4 and d_3, d_4. The average state space model is given by equations (1) and (2) [6]. The state variables are the transformer magnetizing current (I_M), the inductance current (I_L), and the dc/dc power converter output voltage (S). The inputs are the source voltage (V_g) and the diodes threshold voltage (V_d). The outputs are the source current (I_G) the current (I_L), and the voltage (S). φ is the duty cycle value, r_p, r_s, L_M, n are respectively primary resistance, secondary resistance, magnetizing inductance and the ratio of the HF transformer. L and r_L are the coil inductance and the coil resistance of the isolated buck converter. r_{mos} is the channel transistor MOSFET resistance. Re and C_e are the resistance and the capacitance of the isolated buck converter. C_{dc} is the DC bus capacity and the load R_{ch} is supposed resistive.

$$A_{mean}(\varphi)=\begin{bmatrix} \frac{R_{mos}.\varphi+R_{mos}+rp}{L_M} & 0 & 0 \\ \frac{n.(2.R_{mos}+rp)}{L} & \frac{r_L+rs.\varphi+n^2.\varphi(2.R_{mos}+rp)}{L} & -1/L \\ 0 & 1/C_{eq} & -1/R_{eq}.C_{eq} \end{bmatrix}$$

$$B_{mean}(\varphi)=\begin{bmatrix} 0 & 0 \\ \frac{n.\varphi}{L} & -\frac{2}{L} \\ 0 & 0 \end{bmatrix}, \quad C_{mean}(\varphi)=\begin{bmatrix} \varphi & n.\varphi & 0 \\ 0 & 1 & 0 \\ 0 & 0 & 1 \end{bmatrix} \qquad (1)$$

with:

$$\frac{1}{R_{eq}}=\overline{M}\frac{1}{R_e}+M\frac{R_e+R_{ch}}{R_eR_{ch}}, \quad \frac{1}{C_{eq}}=\overline{M}\frac{1}{C_e}+M\frac{1}{C_e+C_{dc}} \qquad (2)$$

Let also refer to entry in row i and column j for matrix $A_{mean}(\varphi)$ (resp. $B_{mean}(\varphi)$ and $C_{mean}(\varphi)$) as a(φ, i, j) (resp. b(φ, i, j) and c(φ, i, j)). The average output voltage S is obtained from the balance state of the average model:

$$S = n.\varphi.V_g - 2.V_d - [r_L + r_s.\varphi + n^2.\varphi.(2Rmos + r_p)].i_L \qquad (3)$$

C. Multimodel of two coupled dc/dc converters

A multimodel of the coupling of several dc/dc power converters can be deduced from equation (1) to (3) [6]. For simplicity, this multimodel is detailed in case of two identical dc/dc power converters. The hybrid system, considered, has two energy sources: a photovoltaic module (source 2) [15] and a storage battery bank (source 1) [16], [17] to ensure the service continuity. For this system, two contactors (M_1, M_2) are required; and four configurations (mode 1 to mode 4) may occur. The resulting multimodel is given by (4) and (5). The state vector is $X = [I_{M1}, I_{L1}, I_{M2}, I_{L2}, S_1, S_2]^T$, the output vector is $Y = [Ig_1, I_{L1}, Ig_2, I_{L2}, S_1, S_2]^T$ and the input vectors is $U = [Vg_1, Vd_1, Vg_2, Vd_2]^T$. The sub-matrices 1 and 2 correspond to the internal variables of the ZVS full bridge isolated buck converters 1 and 2. The two last rows of the state matrix correspond respectively to the coupling equations of the dc / dc converters 1 and 2 on the dc bus. The structure of the matrices A_{mean} changes according to the configuration (i.e. the states of the contactors M_1 and M_2).

$$A_{mean}(\varphi_1,\varphi_2)=\begin{bmatrix} a(\varphi_1,1,1) & a(\varphi_1,1,2) & 0 & 0 & 0 & 0 \\ a(\varphi_1,2,1) & a(\varphi_1,2,2) & 0 & 0 & a(\varphi_1,2,3) & 0 \\ 0 & 0 & a(\varphi_2,1,1) & a(\varphi_2,1,2) & 0 & 0 \\ 0 & 0 & a(\varphi_2,2,1) & a(\varphi_2,2,2) & 0 & a(\varphi_2,2,3) \\ 0 & \frac{1}{C_{eq1}} & 0 & M_1M_2\frac{1}{C_{eq1}} & \frac{-1}{(R_{eq1}C_{eq1})} & 0 \\ 0 & M_2M_1\frac{1}{C_{eq2}} & 0 & \frac{1}{C_{eq2}} & 0 & \frac{-1}{(R_{eq2}C_{eq2})} \end{bmatrix}$$

$$B_{mean}(\varphi_1,\varphi_2)=\begin{bmatrix} b(\varphi_1,1,1) & b(\varphi_1,1,2) & 0 & 0 \\ b(\varphi_1,2,1) & b(\varphi_1,2,2) & 0 & 0 \\ 0 & 0 & b(\varphi_2,1,1) & b(\varphi_2,1,2) \\ 0 & 0 & b(\varphi_2,2,1) & b(\varphi_2,2,2) \\ 0 & 0 & 0 & 0 \\ 0 & 0 & 0 & 0 \end{bmatrix}$$

$$C_{mean}(\varphi_1,\varphi_2)=\begin{bmatrix} c(\varphi_1,1,1) & c(\varphi_1,1,2) & 0 & 0 & 0 & 0 \\ c(\varphi_1,2,1) & c(\varphi_1,2,2) & 0 & 0 & 0 & 0 \\ 0 & 0 & c(\varphi_2,1,1) & c(\varphi_2,1,2) & 0 & 0 \\ 0 & 0 & c(\varphi_2,2,1) & c(\varphi_2,2,2) & 0 & 0 \\ 0 & 0 & 0 & 0 & 1 & 0 \\ 0 & 0 & 0 & 0 & 0 & 1 \end{bmatrix} \quad (4)$$

with:

$$\frac{1}{C_{eq1}}=M_2\overline{M_1}\frac{1}{C_e}+\overline{M_2}M_1\frac{1}{C_e+C_{dc}}+M_2M_1\frac{1}{2C_e+C_{dc}}+\overline{M_2}\,\overline{M_1}\frac{1}{C_e}$$

$$\frac{1}{R_{eq1}}=M_2\overline{M_1}\frac{1}{R_e}+\overline{M_2}M_1\frac{R_e+R_{ch}}{R_eR_{ch}}+M_2M_1\frac{R_e+2R_{ch}}{R_eR_{ch}}+\overline{M_2}\,\overline{M_1}\frac{1}{R_e}$$

$$\frac{1}{C_{eq2}}=M_2\overline{M_1}\frac{1}{C_e+C_{dc}}+\overline{M_2}M_1\frac{1}{C_e}+M_2M_1\frac{1}{2C_e+C_{dc}}+\overline{M_2}\,\overline{M_1}\frac{1}{C_e}$$

$$\frac{1}{R_{eq2}}=\overline{M_2}M_1\frac{1}{R_e}+M_2\overline{M_1}\frac{R_e+R_{ch}}{R_eR_{ch}}+M_2M_1\frac{R_e+2R_{ch}}{R_eR_{ch}}+\overline{M_2}\,\overline{M_1}\frac{1}{R_e} \quad (5)$$

III. SUPERVISORY CONTROL WITH PETRI NETS

The capability of the hybrid energy systems to satisfy the power demand depends on the atmospheric conditions. Basically, it is possible to control the power delivered to the load, under the constraint that the voltage level on the dc bus is constant (V_{ref}) whatever the sources and load variations, by controlling the current provided by each source. The operating modes are then determined by the energy balance between the total generation (solar + battery bank for the example detailed in II.c) and the load demand (for simplicity, the recharge cycle of the battery bank is not considered in this work).

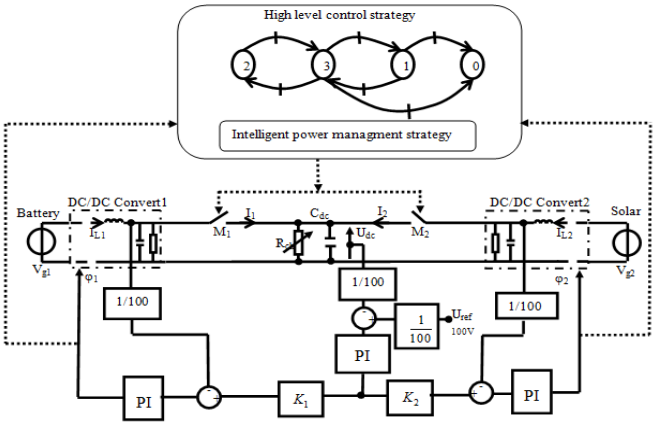

Fig.3: Supervisory control design for a two sources hybrid energy system

Petri nets are introduced in this section in order to propose a supervisory control of the hybrid energy system. This controller is based on the duty cycle variables which control the dc/dc power converters. It selects the coupled sources onto the dc bus according to available renewable energy and load fluctuations. Then, it drives also the power ratio between these sources in order to manage efficiently the operations of the generation subsystems. Fig. 3 shows the controller for the case of a two sources hybrid systems (see the example detailed in II.c). The high level is a PN that selects the operating mode (section III.B). The low level is a local controller that manages the power ratio between the sources that are coupled in a given mode and drives the current and voltages for each converter (sections III.C to III.E). The supervisory control drives two sets of variables: discrete variables relative to the switching of M1 and M2 (high level), and continuous variables corresponding to the adjusted gains K_1 and K_2 (between 0% and 100%) that make it possible to control the ratio of current provided by each source whenever the sources are both connected onto the dc bus (low level).

A. Petri nets

An ordinary Petri net (PN) with n places and q transitions is defined as < P, T, Pre, Post > where P={P_i} is a finite set of places and T={T_j} is a finite set of transitions. $W_{PR} = (w^{PR}_{ij}) \in \{0, 1\}^{n \times q}$ with w^{PR}_{ij} = Pre (P_i, T_j) (i.e. weight of the arc from place P_i to transition T_j) is the pre-incidence matrix. $W_{PO} = (w^{PO}_{ij}) \in \{0, 1\}^{n \times q}$ with w^{PO}_{ij} = Post (P_i, T_j) (i.e. weight of the arc from transition T_j to place P_i) is the post-incidence matrix. The PN incidence matrix W is defined as $W = W_{PO} - W_{PR}$ [18], [24]. $M = (m_i) \in (\mathbf{Z}^+)^n$ is the marking vector and $M_I \in (\mathbf{Z}^+)^n$ the initial marking vector, with $\mathbf{Z}^+$ the set of non negative integer numbers. A firing sequence σ is defined as an ordered series of transitions that are successively fired from marking M to marking M'. Such a sequence σ is represented by its characteristic vector (i.e. Parikh vector) $X = (x_j) \in (\mathbf{Z}^+)^q$ where x_j stands for the number of times T_j has occurred in sequence σ. The marking M' resulting from the marking M with the execution of the sequence σ is given by $\Delta M = M' - M = W.X$.

B. High level part of the controller

Because of its variable structure, the hybrid power distributed generation system has four possible operating modes. The aim of the high level part of the controller is to switch from one mode to another according to the climatic condition, the state of charge of the battery bank and the load variation. The commutations between the modes are given according to the following rules:

Mode 0: All sources are disconnected onto the dc bus. This situation avoids damages and occurs when there is no sufficient solar power and when the state of charge (SOC) of the battery is also very low. For the following, the starting from mode 0 will be manual and is not further investigated.

Mode 1: This mode corresponds to a situation in which only the battery bank is used to track a power reference while the solar subsystem is disconnected. This situation is maintained while the state of charge exceeds the threshold SOCmin or until the power available with solar subsystem exceeds a threshold power. Beyond those limits, the system must switch to Mode 0 or Mode 3.

Mode 2: This mode corresponds to periods of sufficient PV power to satisfy the total demand. Therefore, the PV subsystem has to track the total demand while the battery bank is storing energy following the recharge cycle. For simplicity, the recharge policy is not studied in this paper. This situation is maintained until the total power demand does not exceed the maximum available PV power. When this condition is no longer satisfied, the system switches to Mode 3.

Mode 3: This mode is characterized by the coupling of both generation subsystems. Note that operation in Mode 3 can be maintained as long as the energy available in the battery bank is sufficient to complement the PV generation in order to satisfy the load requirements. If this limit is surpassed, the load and the sources must be disconnected.

The PN controller (fig. 4, central part) drives the modes commutations according to the state of charge of the battery bank (fig. 4, left part) and to the magnitude of solar radiation (fig. 4, right part). The central part (P_1 to P_4 and T_1 to T_6) of the PN in figure 4 drives the modes commutations. Each mode is represented by a single place: P_1 stands for mode 0, P_2 for mode 1, P_3 for mode 3, and P_4 for mode 2. As a consequence, the position of the token in central subnet is an indicator of the renewable energy penetration that increases from the right to the left. The left part (P_5 to P_6 and T_7 to T_8) of the PN in figure 4 stands for the state of charge of the battery bank in comparison with the load demand. A token in place P_5 represents a low level whereas a token in place P_6 represents a high level. The right part (P_7 to P_9 and T_9 to T_{12}) of the PN in figure 4 stands for the climatic conditions to use the solar panel. A token in place P_7 represents a low magnitude of the solar radiations whereas a token in place P_9 represents a high one (in comparison with the load demand).

The use of PN as a high level controller is motivated at first in order to deal with the discrete dynamics of the modes switching in SMSE. One can notice that automata or final state machines are also suitable for that purpose [22]. Anyway, one challenging issue with PN is the possibility to include the low level parts of the controller (section III.C to III.E) by introducing hybrid PN [26] in order to include all control components in a framework. Moreover, numerous results exist for the analysis and control of hybrid systems based not only on discrete PN but also on continuous and hybrid ones [26]. As a consequence, the use of continuous and hybrid PN to control multisource energy systems may be further investigated.

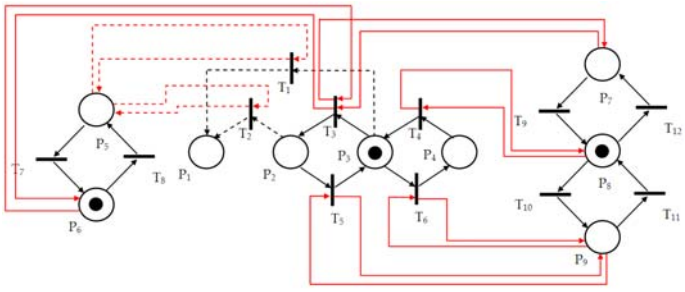

Fig. 4: PN controller (dotted lines concern the mode 0)

C. *Sensorless approach for the modes commutations*

The decision criteria used to switch the sources is based on the duty cycle variables which control the dc / dc power converters. We will show that the duty cycle value acts as a virtual sensor and is an efficient indicator of the correlation between the sources and load. The advantage of our method is that it is based on indirect measurement and does not require any additive sensor (in comparison of usual strategies that use direct measurements of available power of the sources [2], [4]). Another advantage is that it could be easily generalized to other sources with the same set of variables (wind turbines for example).

Our method exploits the property that the duty cycle value increases if the voltage source decreases. The high level control strategy has to decide which operating mode must be used according to some thresholds that concern the duty cycle value. The table 1 sums up the conditions to be satisfied to couple or uncouple the sources onto the dc bus. These conditions will be used as logical firing conditions for the PN controller (fig. 4).

	Type	**Conditions / Parameters**
T_1	Timed	0.1 TU
T_2	Timed	0.1 TU
T_3	Timed	0.1 TU
T_4	Timed	0.1 TU
T_5	Timed	0.1 TU
T_6	Timed	0.1 TU
T_7	Immediate	$\varphi bat \leq \varphi batseuil_{max}$ (0.8)
T_8	Immediate	$\varphi bat \geq \varphi bat_{max}$ (0.9)
T_9	Immediate	$\varphi solestime \leq \varphi solseuil_{max}$ (0.8)
T_{10}	Immediate	$\varphi solestime \leq \varphi solseuil_{min}$ (0.4)
T_{11}	Immediate	$\varphi sol \geq \varphi solseuil_{max}$ (0.8)
T_{12}	Immediate	$\varphi sol \geq \varphi sol_{max}$ (0.9)

Table 1: Firing conditions of the transitions

φsolestime is an estimation of the duty cycle value of the PV when the system is in mode 1 (PV source is disconnected):

$$\varphi solestime = \frac{\left(S + 2.V_d + r_L.i_L\right)}{n.V_g - \left(r_s + n^2.(2.Rmos + r_p)\right).i_L} \quad (6)$$

D. *Energy ratio balance*

The decision criteria based on duty cycle is also useful to drive the energy ratio between the sources when several sources are simultaneously coupled onto the dc bus. In the case of the example detailed in section II.c, the duty cycle is used to determine the energy ratio, between the PV and the battery while satisfying the power demand. This ratio depends on the gains K_1 and K_2 such that $K_1 + K_2 = 1$. A linear mapping is proposed to drive these gains according to the duty cycle:

$$K_2 = a\varphi_2 + b \quad (7)$$

with a = - 1/ ($\varphi solseuil_{max}$ - $\varphi solseuil_{min}$), and b = $\varphi solseuil_{max}$ / ($\varphi solseuil_{max}$ - $\varphi solseuil_{min}$).

E. Current and voltage local controllers

It is possible to control the power delivered to the load, under the constraint that the voltage level on the dc bus is constant, by controlling the current provided by each source. The multimodel presented in section II is an efficient support for the design of the low level controller (fig. 5) which regulates the voltage on the dc bus (U_{dc}) by driving the current provided by each source and as a consequence the duty cycle of each converter.

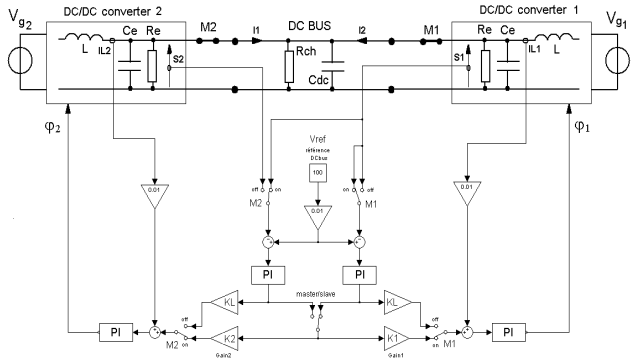

Fig.5: Current and voltage local controllers.

The regulation has a global voltage control loop associated to two local current control loops. Each regulation control loop uses a PI controller whose parameters could be tuned thanks to the model.

IV. SIMULATION RESULTS.

In this section, simulations are proposed using a topology which combined photovoltaic and lead acid battery system, as detailed in section II.c. The proposed PV system is connected to the dc bus via a dc / dc converter. The features of the proposed strategy are studied through an example, which combines periods of sufficient and insufficient generation (fig 6, the load is defined according to its resistance). For simplicity, the PV energy is supposed to be constant. Simulation results are obtained for a time interval between 0 and 10 time units (TU). Simulation results are obtained by developing a detailed MATLAB - SIMULINK package using the mathematical and electrical models of the system described earlier.

The figures 7 to 11 illustrate the performance of our strategy. Fig. 7 illustrates the decisions given by the high level part of the PN controller that result in mode commutations. A delay of 0.1 TU has been introduced to avoid rapid fluctuations due to the transient signals converters (timed transitions in PN model). Fig. 8 depicts the evolution of gains K_1 for the battery and K_2 for the PV to manage the energy flow. Fig. 9 depicts the evolution of the duty cycle for the two sources. In mode 2 the duty cycle value of the converter associated with solar panel is adjusted according to the variable load while the duty cycle of the battery is constant. When this value reaches an upper bound (0.8), the PN drives the system to mode 3.

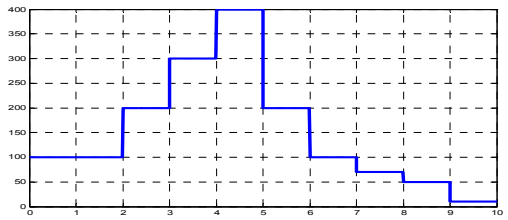

Fig. 6: Load profile (Ω) in function of the time (TU)

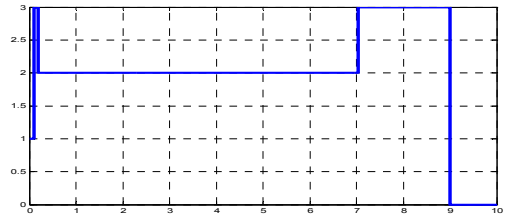

Fig. 7: High level controller: modes switches in function of the time (TU)

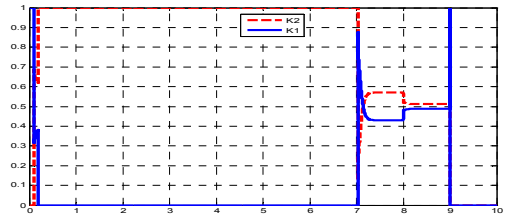

Fig.8: Low level controller: gains K_1 (full line) and K_2 (dotted line) (%) in function of the time (TU)

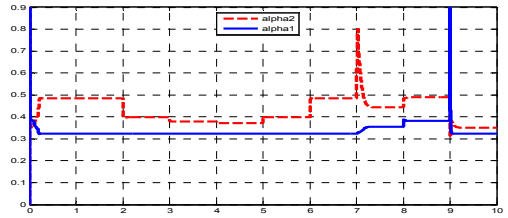

Fig. 9: Duty cycle values: solar (dotted line) and lead acid battery (full line) in function of the time (TU)

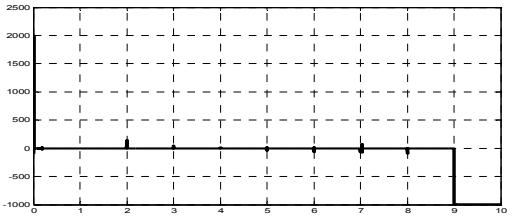

Fig. 10: Power balance in function of the time (TU).

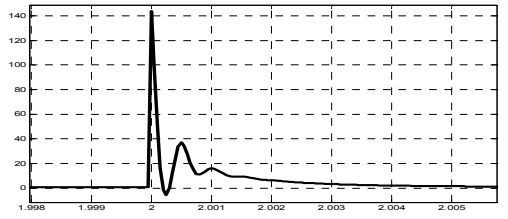

Fig. 11: Perturbation on power balance due to load abrupt variation

In conclusion one can notice that the generated power tracks the total power demand. Figures 10 and 11 show the power balance during the simulation, it can be appreciated

that the results are highly correlated with the profile load. Fig. 11 highlights the instability due to the sudden variations of the load during simulation.

The previous results are compared with the usual method used to drive the hybrid system based on direct measurements on electrical devices or solar radiation (table 2) [2], [4]. With direct measurement, the penetration rate is about 5% higher but, in comparison, our method doesn't need extra sensors and leads to reduced design and exploitation costs. The improvements with direct measurements concerns at most the determination of gains K_1 and K_2 in mode 3 that are directly obtained by measuring the available power of the sources and evaluating the state of charge of the battery bank.

Method	Indirect measurements (φ)	Direct measurements
Mode 0	9.93%	9.99%
Mode 1	1%	1%
Mode 2	68.28%	68%
Mode 3	20.78%	21%
Penetration rate	79.34%	84.01%

Table 2: Performance evaluation

V. CONCLUSIONS AND PROSPECTS

The performance of electric generation multi-source systems relies heavily on the existence of a custom-made high level control capable to efficiently administrate the diverse energy resources involved. The PN control design developed in this paper was proved to be suitable to manage and coordinate the operations of the subsystems that constitute the hybrid energy system by the use of the duty cycle value. It provides decisions to determine the operating mode and the power ratio of each electrical subsystem. The high and low level controllers are designed in a framework so that they cooperate in order to reach the best configuration according to the global control objective assessed of the hybrid system.

Our further works will concern the following questions. A generalization of the PN controller to several sources will be considered and a supervisory control will be designed for the management of complex power hybrid systems. To improve the penetration rate, we will also continue our study about the use of the duty cycle and we will propose a more accurate mapping to tune the gains K_i. Non linear and fuzzy mappings would be investigated to improve the relationship (7). At last, the proposed strategy will be implemented and validated on our experimental technologic center in Fecamp.

REFERENCES

[1] R.Chedid, H. Akiki and S. Rahman - "A decision support technique for the design of hybrid solar-wind power systems" - *IEEE TEC*, Vol. 13, No. 1, 1998.

[2] A. de Lemos Pereira "Modular supervisory controller for hybrid power systems" Risø National Laboratory, Roskilde,2000

[3] X. D. Koutsoukos, P. J. Antsaklis, J. A. Stiver, M. D. Lemmon, "Supervisory Control of Hybrid Systems", Support of the National Science Foundation (ECS95-31485) and the Army Research.

[4] F. Valenciaga and P. F. Puleston, "Supervisor Control for a Stand-Alone Hybrid Generation system Using Wind and Photovoltaic Energy". *IEEE TEC*, Vol.20, No.2, 2005.

[5] J. Lygeros, "Hierarchical, Hybrid Control of Large Scale Systems". UCB-ITS-PRR-96-23 California PATH Research Report. 1996.

[6] A. B. Mboup, F. Guerin, Pape Ndiaye and D. Lefebvre "Multimodel for the coupling of several dc/dc power converters on a dc bus". *IEEE-ISIE 2008,* Cambridge (GB), 2008

[7] E. Pepa, "Adaptive Control of a Step-Up Full-Bridge DC-DC Converter for Variable Low Input Voltage Applications" - Phd thesis of the Virginia Polytechnic Institute and State University.

[8] J. A. Sabate, V. Vlatkovic, R. B. Ridley, F. C. Lee, and B. H. Cho, "Design considerations for high-voltage high-power full-bridge zero voltage-switched PWM converter"- *Proc. IEEE APECE* - pp. 275–284, 1990.

[9] S.-J. Jeon and G.-H. Cho, "A zero-voltage and zero-current switching full bridge DC-DC converter with transformer isolation" - *IEEE Trans. Power Electron.*, vol. 16, no. 5, pp. 573–580, 2001.

[10] R. W. Erickson, "DC-DC Power Converters" - Department of Electrical and Computer Engineering University of Colorado Boulder, CO 80309-0425, *Wiley Ency. of Elect. and Electronics Eng.*.

[11] P.Z.Lin, C.M. Lin, C.F. Hsu and T. T. Lee, "Type-2 fuzzy controller design using a sliding-mode approach for application to DC-DC converters" - *IEE Proc-Electr.power Appl.*, Vol.152, No.6, 2005.

[12] J.Sun and H. Grotstollen, "Symbolic analysis method for average modeling of switching powers converters" - *IEEE TPE*, 12, 1997.

[13] M. Ashari† and C. V. Nayar, "An optimum dispatch strategy using set points for a photovoltaic (PV)–diesel–battery hybrid power system" *Solar Energy*, Elsevier Science Ltd, Vol. 66, No. 1, pp. 1–9, 1999.

[14] R. Dufo-Lopez,, J.´ L. Bernal-Agustın, "Design and control strategies of PV-Diesel systems using genetic algorithms." *Solar Energy* 79 33–46, 2005.

[15] G. Walker, "Evaluating mppt converter topologies using a matlab pv model" - Dept of Computer Science and Electrical Engineering, University of Queensland, Australia.

[16] M.El Mokadem, C. Nichita, G.Barakat and B.Dakyo, "Control strategy for stand alone wind-diesel hybrid system using a wind speed model" - *Electrimacs* 18-21, 2002.

[17] P. Bastard, F-X. Vallet, Simulation du démarrage à froid des véhicules automobiles - Pôle Calcul Service « Etudes Electrotechniques », Direction de l'Electronique Avancée (DEA)

[18] R.G. Askin, C. R. Standridge, *Modeling and analysis of Petri nets*, John Wiley and sons Inc., 1993.

[19] G.W. Brams, *Réseaux de Petri, Vol I et II*, Masson, Paris, 1983.

[20] W. Brauer W. Reisig, G. Rozenberg, Petri nets: Central models and their properties, *Lecture Notes in Compt. Sci.,* vol. 254, Springer Verlag. 1986.

[21] C.G. Cassandras, *Discrete event systems: modeling and performances analysis*, Kluwer Academic Publishers, 1998

[22]-C.G. Cassandras, S. Lafortune, *Introduction to Discrete Event Systems*, 2nd Edition, Springer, 2007.

[23] A. Giua, F. DiCesare, Petri net structural analysis for supervisory control., *IEEE Trans. on Robotics and Automation*, Vol. 10, No. 2, pages 185-195, 1994.

[24] T. Murata, Petri nets: properties, analysis and applications, *Proceedings IEEE*, vol.77, no. 4, pp 541-580, 1989.

[25] P.J. Ramadge, W.M. Wonham, Supervisory control of a class of discrete event processes, *SIAM J. Cont. Opt*., vol. 25, pp. 206-230, 1987.

[26] M. Silva, L. Recalde, On fluidification of Petri Nets: from discrete to hybrid and continuous models , *Annual Reviews in Control*, Vol. 28, no. 2, pp. 253-266. 2004.

[27] M. Uzam, A.H.Jone, I. Yucel, I, A rule-based methodology for supervisory control of discrete event systems modeled as automation Petri nets, *Int. J. of Int. Cont. Syst.*, vol. 3, no. 3, pp. 297-325, 1999.

[28] J. Zaytoon, (éditeur), Hybrid dynamical systems, *APII - JESA*, vol 32, n° 9-10, 1998.

[29] T. Tafticht, K. Atif, and K. Agbossou, Utilisation des Réseaux de Petri pour la Modélisation du Convertisseur MPPT d'un Système Photovoltaïque, *IEEE - CCECE*, vol. 1, no. 4-7, pp. 543–546, 2003.

[30] J. R. B. Sousa, A. M. N. Lima, Modeling and Simulation of Systems of Multiple sources of Energy by Differential Hybrid Petri Nets, *IEEE-ISIE*, pp1861 – 1866 , Cambridge (GB), 2008.

[31] V K. Paruchuri, A. Davari, and A. Feliachi, "Hybrid Modeling of Power System using Hybrid Petri nets," *SSST'05*, pp. 221–224, 2005.